EFFECT OF ARTIFICIAL AGING TREATMENT ON MICROSTRUCTURE, MECHANICAL PROPERTIES AND FRACTURE BEHAVIOR OF 2017A ALLOY

Nassim Aguechari[1,2], Achraf Boudiaf[3], Mohand Ould Ouali[1]*

[1]Laboratory Elaboration and Characterization of Materials and Modelling (LEC2M), University Mouloud MAMMERI of Tizi-Ouzou, Algeria.
[2]Centre de Développement des Satellites (CDS), Agence Spatiale Algérienne. Oran, Algeria.
[3]Laboratoire Génie des Matériaux, École Militaire Polytechnique, Bordj-El-Bahri, Algeria.

Abstract

The effect of artificial aging treatment on 2017A aluminum alloy microstructure, mechanical properties, and fracture behavior was investigated. The samples were taken from the as-received alloy and aged at 170 °C for 5, 10, 15, 20, and 30 hours. An optical microscope, scanning electron microscope (SEM), X-ray diffraction (XRD), microhardness and tensile strength tests were used to characterize mechanical and microstructural properties. The microstructural analysis revealed that as the aging treatment duration is increased, the size and density of precipitates grow larger and more numerous. According to X-ray diffraction measurements, the microstructural evolution caused by aging treatments is primarily due to an increase in precipitation of the hardening phase θ-Al_2Cu. According to the tensile test results, the yield stress increases with increasing aging duration. The fracture surface analysis of failed specimens subjected to tensile loading revealed that the aging treatment conditions had a significant impact on the morphology and mode of fracture: the mixed-mode (ductile-brittle) failure was established for intermediate aging durations (aging at 170 °C for 15 and 20 h), and the intergranular fracture was found to be more pronounced when the aging duration is prolonged due to the coalescence of fine precipitates at the grain boundary.

Keywords: 2017A aluminium alloy; aging; microstructure; mechanical properties; fracture mechanism.

---

[*] Corresponding author: Nassim Aguechari, *aguecharinassim.pg@gmail.com*

Introduction

Despite the growth and technological progress recorded in the last 20 years in the development of composite materials, aluminum alloys are the most commonly used in civil and military aircraft structures. Several properties such as high strength/weight ratio, ductility, good fracture toughness, machinability and reasonable cost make this type of alloy a perfect choice for aerospace engineers [1-4]. Among Al alloys, Al-Cu-based alloys (2xxx series) have been widely used in the aerospace industry for the wings and fuselage skins of the planes, particularly the 2017A and 2024 which are the earliest alloys used on aircraft [5, 6]. Generally, these alloys are used in the form of wrought sheet and plate forms. Al-Cu based alloys are usually strengthened by precipitation hardening treatment which involves three steps: (1) Solution treatment to generate a homogeneous solid solution (α), the θ precipitates are dissolved in the Al matrix, (2) rapid quenching forming a supersaturated solid solution of α_{ss} which contains excess copper, (3) aging is the process of precipitating incoherent precipitates from a supersaturated solid solution. The fine precipitates in the alloy block dislocation movement. By impeding the dislocation movement during deformation, the alloy is strengthened. For Al-Cu based alloy, the precipitation sequence is based on the formation of the first coherent phase called a GP (Guinier Preston) zone which is then followed by intermediate coherent (θ'') and semi-coherent (θ') phases before the stable $\theta(Al_2Cu)$ phase. The precipitation reaction during the aging process for an Al-Cu alloy, such as 2017A is quite complex or/and not well defined in the literature, but can be generally described as follows [7-10]:

$$\alpha_{ss} \rightarrow GP\ Zones \rightarrow \theta' \rightarrow \theta'' \rightarrow \theta\ (Al_2Cu)$$
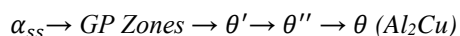
Precipitation hardening treatment generates different microstructures; the mechanical properties of the based Al-Cu alloys are strongly dependent on the nature of the microstructure obtained after treatment i.e. the type, size, coherency, spacing and distribution of the precipitates in the microstructure impact strength evolution of the material [8,11].

The use of aluminum alloys in aeronautics requires particular requirements knowing that structures are designed to keep their integrity for a longer lifetime and under high-temperature conditions. In addition to changes in the microstructure (nucleation and growth of cavities, formation of microcracks and dislocations ...) due to the manufacturing process of materials, the thermo-mechanical treatments and in-service conditions [12-13], the mechanical and physical properties of an aluminum alloy can be changed because of the material microstructure evolution during long-term service. Such changes can cause premature material degradation. Aging or "accelerated aging" is one of the experimental methods used to assess the degradation of materials, namely aluminum alloy, exposed to the long-term service environment such as aircraft structures, electrical wires, etc. [14-16].

In the literature, the effects of aging on the evolution of microstructure and its influence on the mechanical properties of the based Al-Cu-Mg (mainly 2017A and 2024) alloys are widely investigated [16-19]. In these studies, "aging" was considered as a tempering treatment realized after solution treatment and quenching. *Bayarassou et al.* studied the microstructures and mechanical properties changes during aging and homogenization treatment of Al-Mg-Si alloy wire cold drawn at the different deformations [16]. *Radutoiu et al.* were interested in the influence of the artificial

over-aging time to hardness and mechanical properties of an A2024 alloy, measured by nanoindentation. Hemmouche and co-authors were interested in the coupled effects of heat treatments and anodizing processes on the fatigue life of aluminum alloy 2017A [18-19]. *Larignon et al and Prudhomme et al.* observed a high density of intergranular precipitates and significant evolution (modification) of the microstructure for an aging time longer than 55 h at 150 °C [20, 21]. *Alexopoulos* has studied the corrosion-induced mechanical degradation of 2024 aluminum alloy under different artificial aging conditions [22]. He showed that the aging temperature has an impact on the amplitude of mechanical properties of 2024 aluminum alloy aged at 210 °C.

However, most of the studies cited above have been conducted using the 2024 alloy. There is not sufficient and detailed work concerning the effect of artificial aging treatment carried out on 2017A alloy despite its good physical and mechanical properties and its use on aircraft and aerospace structures.

As a complementary work to a better understanding of the microstructure evolution induced by aging and this effect on mechanical properties and fracture mechanism, several experimental techniques were conducted in this work to establish relationships between microstructure, mechanical properties and fracture behavior of the 2017A alloy exposed to different artificial aging treatment conditions. In particular, our contribution is to evaluate microstructural evolution, represented here by the type, size and density of precipitates, induced by aging and its impact on mechanical properties and mechanism of fracture of the material. In this study, the artificial aging treatments are applied on a 2017A sheet alloy from a given metallurgical state. The main aim is to investigate the impact of long-time thermal exposure on microstructure, mechanical properties and fracture behavior of a 2017A-T4 aluminum alloy by considering a pristine (as received) alloy that was consequently artificially aged. In section 2, the material and the experimental techniques and methods used to carry out the study are presented. The results concerning the effect of aging treatment on microstructure evolution, mechanical properties and the fracture mechanism are done and discussed in section 3. A comparison of the results obtained on artificially aged material and those of the pristine (as-received) material is also shown. Concluding remarks and some perspectives are made in the last section.

Material and experimental techniques

The material used in the present study is a heat-treated 2017A-T4 aluminum alloy sheet form with a thickness of 3 mm. The weight percentage chemical composition of the alloy is presented in Table 1.

Table 1. Chemical composition of 2017A-T4 aluminum alloy (wt. %).

Elements	Al	Cu	Mg	Mn	Si	Fe	Cr	Zn
Wt. %	balance	3.53	0.66	0.83	0.7	0.43	0.026	0.1

Artificial aging treatments of samples taken from the as-received 2017A-T4 alloy were carried out at 170 °C for a duration comprised between 0 and 30 h (Table 2). The main reason for selecting this temperature is to exploit the temperature range currently used by the industry in the artificial aging of commercial aluminum sheets form [23]. To assess the effect of aging treatment on microstructure and mechanical properties of

2017A-T4 aluminum alloy, microstructural and mechanical tests were performed on the pristine and aged samples, the results are then compared. All the testing was carried out at room temperature.

The microstructure of the alloy was analyzed using an optical microscope linked with a computerized imaging system equipped with Cyber link software. All the samples are prepared by metallographic grinding with 800, 1000, 1200 and 1500 grit size silicon carbide emery papers and then polishing with 1 μm diamond paste is applied to the top surface to obtain a mirror state. The polished samples were etched in Keller's reagent (95 ml H2O + 3.5 ml HNO3 + 1.5 ml HCl +1 ml HF). The X-ray diffraction analysis was used to identify precipitates at different aging treatment conditions.

The tensile tests were carried out on the EZ20 LLOYD Ametek machine with a strain rate of 2 mm.mn^{-1}. Three samples were tested for tensile properties and the average curves were reported for each case. Specimens were machined in the rolling direction L with CNC machining Center according to the ASTM E8 with a gauge length equal to 32 mm (Fig. 1). The microhardness (Vickers) values were determined using the indentation load of 100 g during 10 s. Average values were reported for a minimum of five reading measurements. The fracture surface was studied by a Phillips FEI QUANTA 600 at the potential range of 25-30 KV. The goal is to characterize the effect of artificial aging treatment on fracture mechanisms.
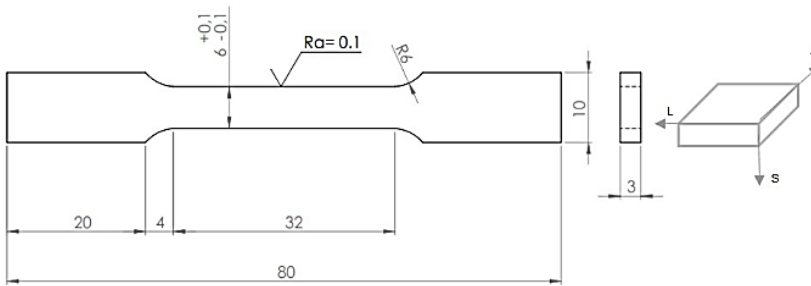

Fig. 1. Geometry and dimensions (in mm) of the tensile samples.

Table 2. Artificial aging treatment conditions of 2017A-T4 aluminum alloy.

Artificial aging treatment at 170 °C
2017A-T4+ 0 h (as-received)
As received + 05 h at 170 °C
As received + 10 h at 170 °C
As received + 15 h at 170 °C
As received + 20 h at 170 °C
As received + 30 h at 170 °C

Results and discussion

1.1.   Effect of aging on microstructure

The microstructure of the pristine material is shown in Figure 2. The optical micrograph shows the multi-phase microstructure of the 2017A-T4 aluminum alloy. This microstructure shows α and θ phases and also the precipitates dispersed throughout the microstructure (Fig. 2(a)), most probably θ' (Al$_2$Cu) which are identified in previous research [6]. The grains exhibit elongation both in the T direction as shown in Figure 2(b).

The X-ray diffraction spectra of 2017A alloy at different aging treatment conditions are shown in Figure 3. Figure 3(a) shows the XRD pattern of the as-received material. In this diffractogram, only four major peaks are observed. They are identified as Al matrix phase, corresponding to planes (111), (200), (220) and (311), respectively. Even though other intermetallic phases are formed but their peaks are not detected. Probably, the absence of other peaks of intermetallic elements is due to the limitation of X-rays in detecting phases with a volume fraction less than 2 %. Figure 3(b-d) shows XRD results from specimens aged at 170 °C for 10, 20 and 30 h respectively. Based on the peaks of graphics, it is proven that the microstructure is composed of Al and Al_2Cu phases. The XRD pattern results are shown in Figure 3(b-d) suggest that the intensity of Al_2Cu precipitates led to an increase after aging treatment.
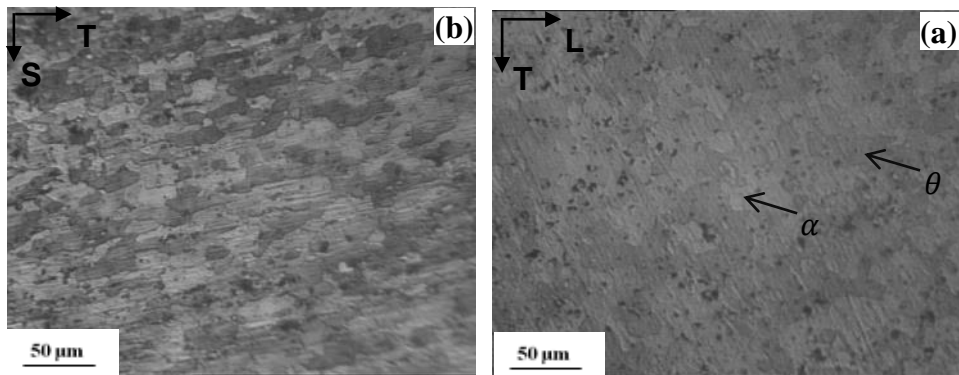

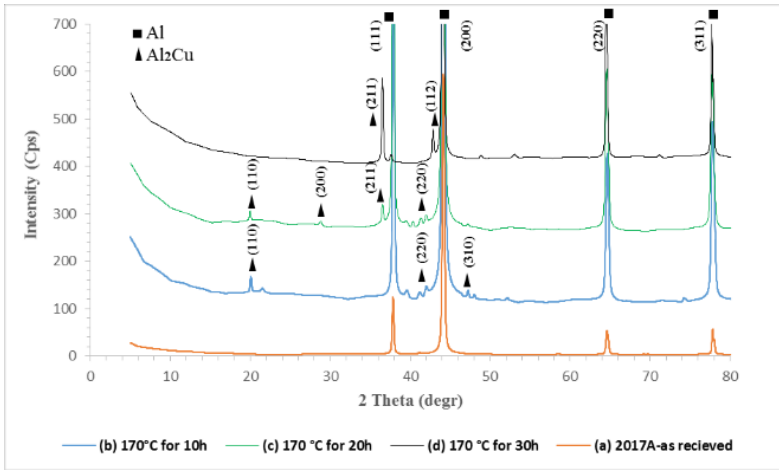*Fig. 2. Optical micrograph of the 2017A-T4 aluminum alloy (as-received material).*

Fig. 3. X-ray diffraction pattern of 2017A alloy under aging treatment at 170 °C for:
(a): as-received material, (b): 10 h, (c): 20 h, and (d): 30 h.

Figures 4 (a-f) show the different microstructures of the 2017A-T4 under different artificial aging conditions as shown in Table 2. According to the OM observation, no significant evolution was observed concerning the coarse intermetallic particles and the grain size for the samples aged at 170 °C for 0, 5 and 10 h (Figs. 4(a-c)).

Although it is difficult to bring out the microstructural evolution of 2017A alloy on this scale of observation, we note, that when the aging duration is increased (Figs. 4(d-f)) the precipitates become larger and more numerous. The presence of block-like particles is expected to be Al-Cu-based intermetallic particles. The composition of these intermetallic particles was found to be Al_2Cu precipitates as indicated by the XRD patterns (Fig. 3) and reported in the literature [25].

It is important to note that the presence of large and numerous precipitates (Figs. 4(d-f)) in the case of aging at 170 °C for 15, 20 and 30 h of duration, is not only due to the exposure of the material to high temperatures as reported in previous work [24] but also to the increase in the duration of exposure that may influence the kinetics of aging.
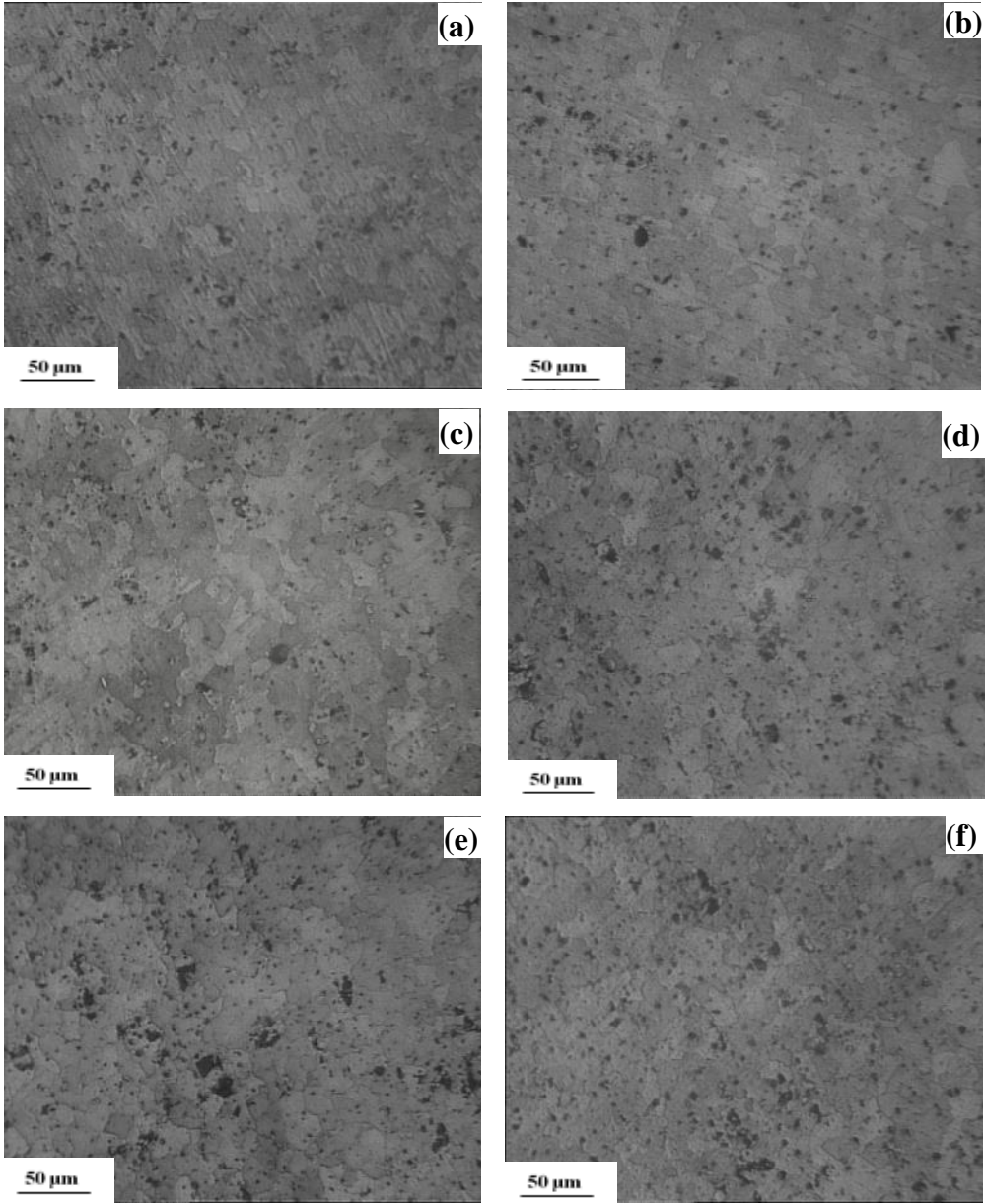
Fig. 4. Optical micrographs of 2017A-T4 alloy aged at 170 °C for different durations:
(a) As received, (b) 5 h, (c) 10 h, (d) 15 h, (e) 20 h, and (f) 30 h.

1.2.   Effect of aging on mechanical properties
        3.2.1   Microhardness
        Microhardness measurements performed on samples artificially aged are represented in Figure 5. The results obtained lead to the same conclusion concerning the effect of aging at 170 °C on the microstructure of the 2017A-T4 alloy. Indeed, aging at 170 °C from 0 to 10 h leads the no significant variations in microhardness which remain stable and less than 135 Hv. Starting from 10h of aging duration, the microhardness increases until reaching its maximum at 150 Hv for 20 h aging treatment, which is frequently considered the result of "peak aging". The increase of microhardness would be due to the formation of GP zones and (θ'', θ') hardening intermediate precipitates [11]. The slight decrease of microhardness at 30 h aging time is due to the reduction of the number and coherency of Al_2Cu precipitates. The results obtained are in agreement with OM and XRD observations, which indicate augmentation of Al_2Cu precipitates from 10 h of aging at 170 °C. Roughly, the results are consistent with the literature data [26, 27].
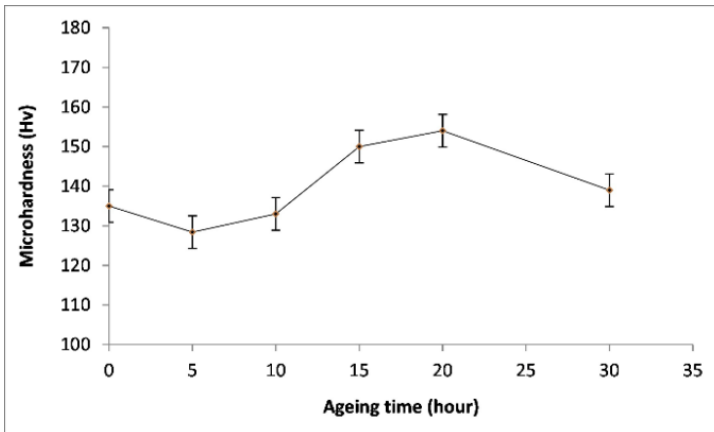

Fig. 5. Microhardness versus the aging time at 170 °C for 2017A-T4 alloy.

3.2.2   Tensile properties measurement
        We show in Figure 6, the stress-strain curve of the 2017A-T4 aluminum alloy under different aging treatment conditions. In this figure, a comparison is done to illustrate the effect of aging time on the mechanical behavior of the aluminum alloy. Figure 7 presents some mechanical properties of 2017A-T4 measured after artificial aging conditions at 170 °C. Yield stress $R_{p\,0.2\,\%}$, maximum stress R_m and elongation at fracture A_f were considered as the main characteristic parameters revealing the microstructure evolution. From 0 to 10h of aging treatment, these three parameters are quite stable (no significant variation of properties).
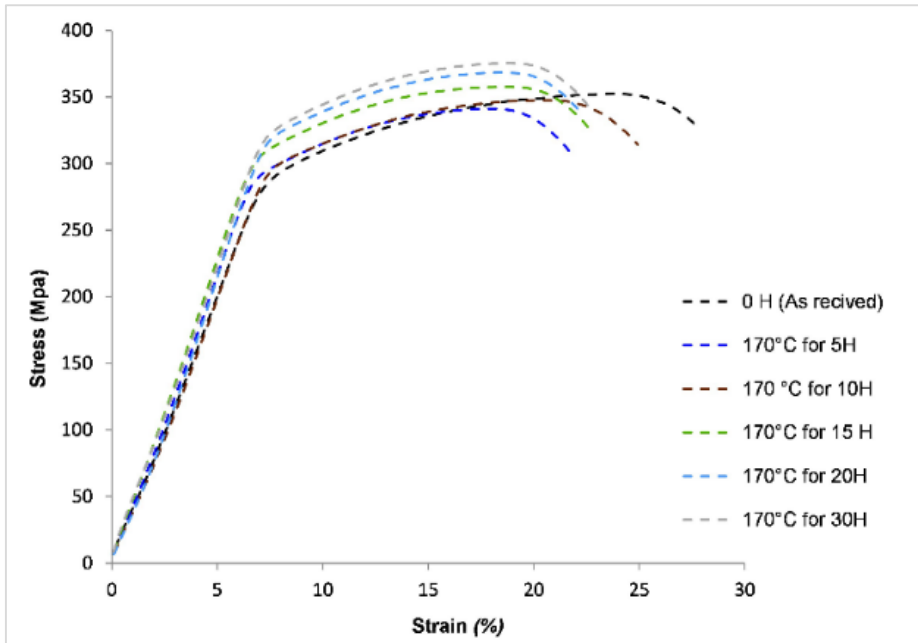
Fig. 6. Stress-strain curves of the 2017A-T4 alloy at different aging conditions.
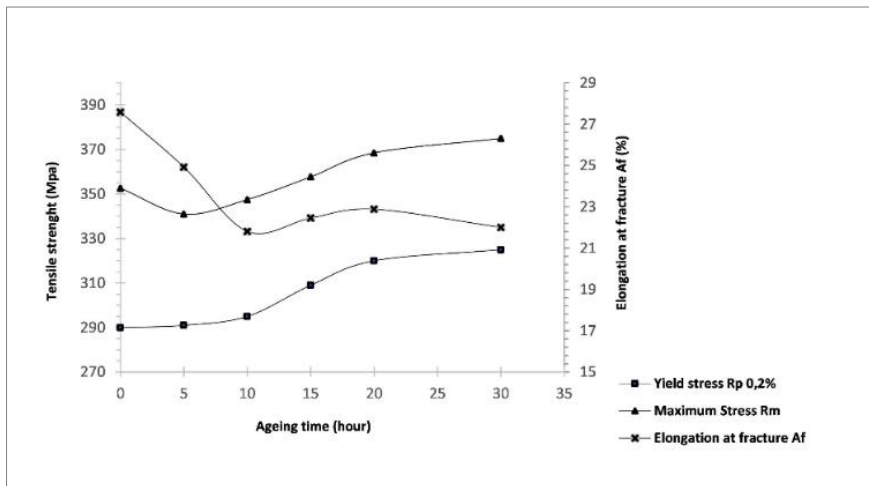

Fig. 7. Mechanical properties of the 2017A-T4 alloy at different aging conditions.

From 10 to 30 h, an increase in maximum stress R_m and yield stress $R_{p\ 0.2\%}$ accompanied by a decrease of elongation at fracture A_f is observed, this is due to the presence of Al$_2$Cu hardening precipitates corresponding to aging at 170 °C for 15, 20 and 30 h of duration. These evolutions reflect a hardening of the structure and can be related to changes in microstructure.

Indeed, taking into account the OM and XRD observations, it is possible to assume that the increase in the yield stress is due to the increase of precipitation of the hardening phase θ-Al_2Cu. However, no significant degradation of the tensile properties is observed compared to the 2017A-T4 pristine material during aging treatment duration (0 to 30 h) at 170 °C.

Effect of aging on fracture behavior

A careful and comprehensive examination of the tensile fractured surfaces can provide useful information. The goal of these analyses is to confirm and assess the impact of the microstructural evolution described above on the fracture mechanism and mode of the 2017A-T4 alloy.
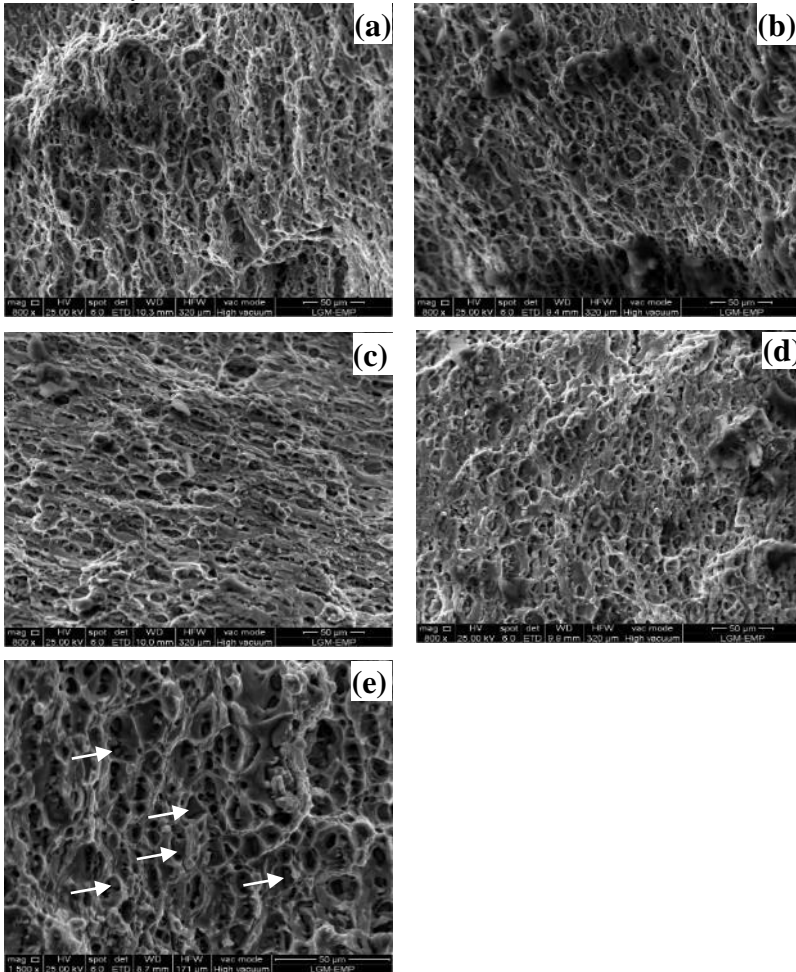

Fig. 8. SEM micrographs of the fracture surface of the 2017A-T4 alloy under aging treatment at 170 °C for: (a): 5 h, (b): 10 h, (c): 15 h, (d): 20 h, and (e): 30 h.

   Figure 8. shows the morphologies of the tensile fracture surface of the 2017A-T4 alloy carried out on samples subjected to different artificial aging conditions. A ductile fracture mode characterized by dimples and voids is observed on the fracture surface for samples aged at 170 °C for 5 and 10 h (Figs. 8(a) and 8(b)). There is no significant change in the failure mechanism and mode to note.

   For the samples aged at 170 °C for 15 and 20 h (Figs. 8(c) and 8(d)), a modification in the morphology of the fracture surfaces is observed. Firstly, less void coalescence is observed on the fracture surface compared to those in Figures 8(a) and 8(b).

   Figures 8(c) and 8(d) indicate the presence of mixed-mode (ductile-brittle) characterized respectively by dimples and platform zone (facets). Magnification in the center of the fracture surface presented in Fig. 8(d) shows a shearing of multiple facets (marked with white arrows in Figure 9(a)). These brittle features at the fracture surface are indicators of the effects of the matrix hardening and the presence of micro-cracks (marked with white discontinuous circles in Figure 9(a)). This phenomenon can be related to the difference in stress concentration between the matrix and the fine dense precipitates of the second phase θ-Al_2Cu.

For 30 h aging treatment, the fracture surface, shown in Figure 8(e), is mainly ductile with a presence of coarse Al_2Cu intermetallic particles (marked with white arrows). These observations are also related in literature [21, 28]. A careful examination of the fracture surface in the center at higher magnifications (Fig. 9(b)) reveals two sizes of voids: The first population of voids is in the size range of 4-10 µm, which were initiated either by fracture or by debonding of the coarse second phase particle of undissolved Al_2Cu particles (marked with a white arrow in Figs. 9(b) and 8(e)).
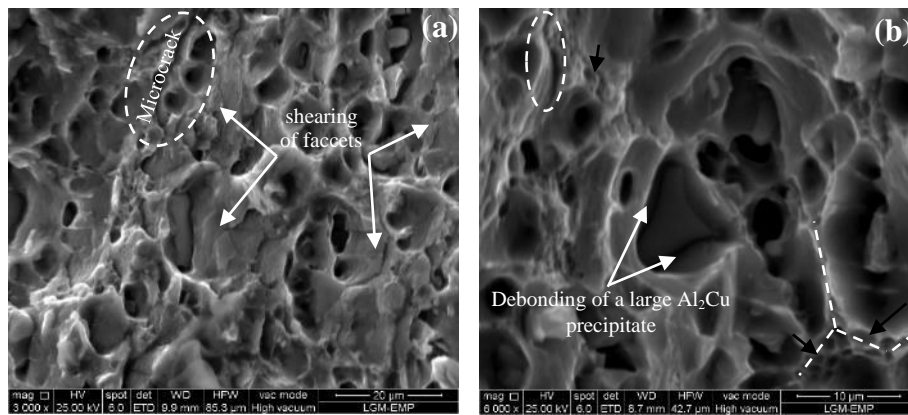

Fig. 9. Fractography at higher Magnification indicates the mechanism of fracture.

   The second population is the microvoids with a size range of 0.5-3 µm (marked with black arrows) located at the grain boundaries as illustrated in Figure 9(b). It is a characteristic feature corresponding to intergranular fracture due to the coalescence of microvoids situated at the grain boundary. When the duration of aging treatment is prolonged, the intergranular fracture surface is predominant due to the presence of numerous and fine intergranular precipitates of θ-Al_2Cu second phase as identified in

[29] on similar alloy (as marked with discontinuous white lines in Fig. 9(b)). The fine precipitation at grain boundaries is a favorable site for the initiation and propagation of micro-cracks (as shown in Fig. 9(b) with a discontinuous white circle).

According to Figure 10. it can be concluded that the mode and mechanism of fracture change with aging treatment conditions; ductile mode with more ductile void coalescence is observed on the fracture surface of samples aged at 170 °C for 0 to 10 h, while the mixed (ductile-brittle) mode with less void coalescence and localized facets is detected on the fracture surface of samples aged at 170 °C for 15 and 20 h, an increase on strength of the material is noticed due to the hardening effect caused by the stress concentration between the interface matrix (α) and θ-Al$_2$Cu precipitates. After 20 h of aging, the mode became ductile with large dimples caused by debonding and/or break off particles (Figs. 8(e) and 9(b)), while the fine precipitates are located at the grain boundary, which initiates ductile intergranular fracture.
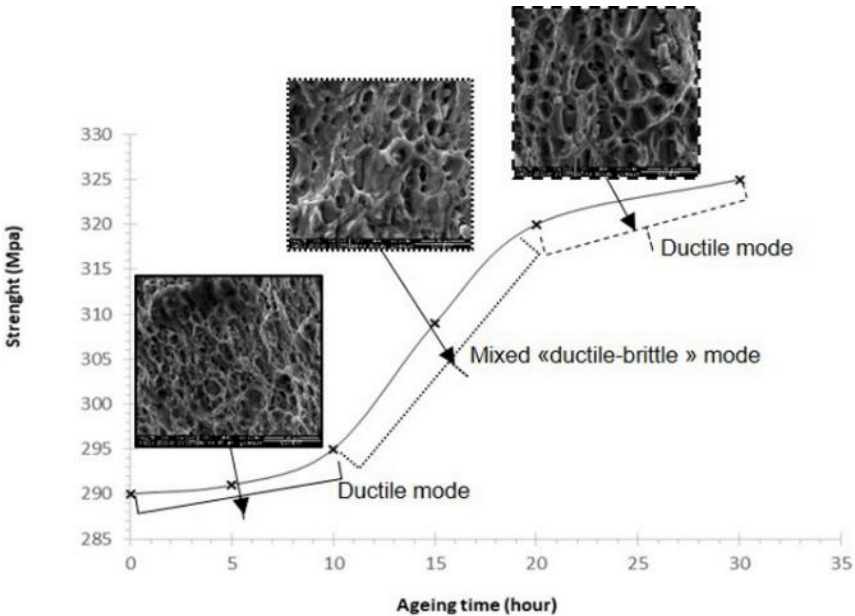

Fig. 10. Summary of the mode of fracture for the tensile samples tested under different aging conditions.

Conclusion

The effect of aging treatment on microstructure, associated mechanical properties and fracture behavior of 2017A alloy were investigated through tensile, microhardness tests and microstructural observations. Key findings from the present study are:

- When the alloy is aged at 170 °C for a duration shorter than 10 h, no significant change in the microstructure is observed, and therefore the mechanical properties remain quite stable.

- After 10 h of aging, an increase of microhardness values is detected until reaching a peak at 20 h of aging duration accompanied by a slight increase of R_m, $R_{p\ 0.2\ \%}$ and a decrease of A_f due to the increase in the intensity of Al$_2$Cu hardening precipitates, which became larger and more numerous when the aging duration is increased.

- The microstructure evolution induced by aging has an impact on morphology and mode of fracture: for the shorter aging duration, the fracture surfaces are mainly ductile, for intermediate aging durations (15 and 20 h), a mixed (ductile-brittle) mode is observed, when the aging duration is prolonged, the fracture mode becomes ductile with characteristic features similar to intergranular fracture due to the fine and numerous intergranular precipitates at the grain boundary.

- Finally, the change detected in microstructure and tensile fracture surfaces of the 2017A exposed to different aging treatments opens the way to exploit other more advanced observation techniques such as the Transmission Electron Microscopy (TEM) to better understand the kinetics of aging. The development of an accelerated aging model capable to predict degradation and damage of the mechanism observed in this paper is claimed. This model aims to describe the behavior of materials exposed to high temperatures for long-life service.

As a perspective of this work, we plan to study the influence of aging on the energy absorption capacity of the material [30-31]. Indeed, the 2017A aluminum alloy is intended for use in structures that can undergo shock loads, an analysis of the failure modes as well as the evolution of the shock absorption capacity will help to optimize the strength of the 2017A alloy.

References

[1] E.A. Starke, J.T. Staley: Progress in Aerospace Sciences, 32 (2-3) (1996) 131-172.

[2] D.G. Altenpohl, Aluminium: Technology, Applications, and Environment, a Profile of a Modern Metal, sixth edition, TMS, Washington, D.C, 1998, 360–364.

[3] T. Dursun and C. Soutis: Materials & Design, 56 (2014) 862-871.

[4] T. R. Prabhu: Acta Metallurgica Sinica (Engl. Lett.), 28 (2015) 909-921.

[5] A. Cochard, J. Douin, B. Warot-Fonrose, J. Huez, L. Robbiola, J-M. Olivier, P. Sciau: Mater. Res. Soc. Symp. Proc, 1656, (2014).

[6] Z. Huda, M. Zaharinie, N.I Taib: Materials Chemistry and Physics, 113 (2009) 515-517.

[7] A. M. A. Mohamed, F. H. Samuel, In: Heat Treatment- Conventional and Novel Applications, (2012) 55-72.

[8] Z. Huda: Int J Mech Mater Eng, 3 (2) (2008) 115-118.

[9] W.G. Frank, M. Goodway: Science, 266 (1994) 1015–1017.

[10] O. B. M. Hardouin Duparc: Metall. Mater. Trans. B, 41 (5) (2010) 1873-1882.

[11] T. R. Prabhu: Eng. Sci. Tech. Int. J, 20 (1) (2016) pp. 133-142.

[12] O. Ostash, V. Uchanin, O. Semenets, Y. Holovatyuk, L. Kovalchuk, V. Derecha: Research in Nondestructive Evaluation, 29 (3) (2017) 156–166.

[13] M. Ould Ouali: Mathematical Problems in Engineering, (2018) Article ID 6454790, 9 pages.

[14]   National Research Council: Accelerated Aging of Materials and Structures: The Effects of Long-Term Elevated-Temperature Exposure, Washington, DC: The National Academies Press, 1996, 29-44.

[15]   M. Bayarassou, M. Zidani, H. Farh: International Journal of Engineering Research in Africa, 36 (2018) 60-68.

[16]   K. Mroczka, A. Wojcicka, P. Kurtyka: Acta Metallurgica Slovaca, 18 (2-3) (2012) 82-91.

[17]   N. Radutoiu, J. Alexis, L. Lacroix, J-A. Petit, M. Abrudeanu, V. Rizea, S. Vulpe: Revista de chimie, 63 (10) (2012) 1042-1045.

[18]   L. Hemmouche, C. Fares, M. A. Belouchrani: Engineering Failure Analysis, 35 (2013) 554–561.

[19]   C. Fares, L. Hemmouche, M. A. Belouchrani, A. Amrouche, D. Chicot, E. S. Puchi-Cabrera: Materials & Design, 86 (2015) 723–734.

[20]   C. Larignon, Mécanismes d'endommagement par corrosion et vieillissement microstructural d'éléments de structure d'aéronef en alliage d'aluminium 2024-T351, Doctorat de l'Université de Toulouse, Institut National Polytechnique de Toulouse, France, 2011.

[21]   M. Prudhomme, F. Billy, J. Alexis, G. Benoit, F. Hamon, C. Larignon, G. Odemer, C.Blanc, G. Hénaff: International Journal of Fatigue, 107 (2018) 60-71.

[22]   N. D. Alexopoulos: Materials Science and Engineering: A, 520 (2009) 40-48.

[23]   J. R. Davis, ASM Specialty Handbook: Aluminum and Aluminum Alloys, ASM International, Ohaio, USA.1993.

[24]   A. Cochard, K. Zhu, S. Joulié, J. Douin, J. Huez, L. Robbiola, P. Sciau, M. Brunet: Materials Science & Engineering: A, 690 (2017) 259-269.

[25]   JANG. J-H, NAM. D-G, PARK. Y-H, PARK. I-M: Transactions of Nonferrous Metals Society of China, 23(3) (2013) 631–635.

[26]   Y-C. Lin, Y-C. Xia, Y-Q. Jiang, H-M. Zhou, L-T. Li: Materials Science & Engineering: A, 565 (2013) 420–429.

[27]   B. Magali, M. Benoit, R-R. Nicolas, D. Christophe, J. Sébastien, W-F. Bénédicte, S. Philippe, D. Joël, DG. Frédéric, D. Alexis: Materialia, 8 (2019) 100429.

[28]   D.A.P. Reis, AA. Couto, N.I. Domingues Jr, AC. Hirschmann, S. Zepka, Carlos de Moura Neto: Defect and Diffusion Forum, 326-328 (2012) 193-198.

[29]   M. Brunet, B. Malard, N. Ratel-Ramond, C. Deshayes, B. Warot-Fonrose, P. Sciau and J. Douin: MATEC Web of Conferences, EDP sciences, 326 (2020) 04007.

[30]   M. Zerouki, M. Ould Ouali, L. Benabou: Metallurgical and Materials Transactions A: Physical Metallurgy and Materials Science, 51(1) (2020) 252-262

[31]   A. Abdul-Latif, A. Ahmed-Ali, R. Baleh, M. Ould Ouali: Thin-Walled Structures, 119 (2017) 332-344